Received: 1 June 2018 | Revised: 10 December 2018 | Accepted: 1 January 2019

DOI: 10.1111/bph.14595

RESEARCH PAPER

Loganetin protects against rhabdomyolysis-induced acute kidney injury by modulating the toll-like receptor 4 signalling pathway

Jie Li[1,2,3*] | Yu-jun Tan[1,2,3*] | Ming-zhi Wang[1,2,3] | Ying Sun[1,2,3] | Guang-yan Li[1,3] | Qi-long Wang[1,2,3] | Jing-chun Yao[1,2,3] | Jiang Yue[5] | Zhong Liu[1,3,4] | Gui-min Zhang[1,3] | Yu-shan Ren[1,3]

[1] Shandong New Time Pharmaceutical Co., Ltd., Lunan Pharmaceutical Group Co., Ltd., Linyi, China

[2] Center for New Drug Safety Evaluation of Lunan Pharmaceutical, Lunan Pharmaceutical Group Co., Ltd., Linyi, China

[3] State Key Laboratory of Generic Manufacture Technology of Chinese Traditional Medicine, Lunan Pharmaceutical Group Co., Ltd., Linyi, China

[4] National Engineering and Technology Research Center of Chirality Pharmaceutical, Lunan Pharmaceutical Group Co., Ltd., Linyi, China

[5] Department of Pharmacology, Wuhan University School of Basic Medical Sciences, Wuhan, China

Correspondence
Dr Yu-shan Ren and Dr Gui-min Zhang, Lunan Pharmaceutical Group Co., Ltd., No. 209 Hongqi Road, Linyi 276006, China.
Email: newtimes2015@yeah.net; lnzhangguimin@lunan.cn

Funding information
National Natural Science Foundation of China, Grant/Award Numbers: 81400752, 81370852, 81270832, 81270833 and 81570674

Background and Purpose: Acute kidney injury (AKI) is a rapid renal dysfunctional disease, for which no effective drugs or therapies are available to improve prognosis. *Loganetin* is a natural product with unknown bioactivities. Here, we identified a new protective effect and mechanism of *Loganetin* in a mouse model of AKI induced by rhabdomyolysis.

Experimental Approach: AKI was induced using glycerol by i.m. injection in mice models. Thirty minutes and 24 and 48 hr after injection of glycerol, the mice received 2 and 18 mg·kg^{-1} of *Loganetin* i.p. respectively. Then mice blood and kidney were collected for various biochemical and histopathological studies. Mechanistic studies on modulation of AKI by *Loganetin* were performed using HK-2 cells and Toll-like receptor 4 (TLR4) knockout mice.

Key Results: In the *Loganetin* treated group, kidney damage and mortality rate were declined, and blood urea nitrogen and serum creatinine were much lower. *Loganetin* prevented damage to the tubular structures induced by glycerol and decreased apoptotic cells at the corticomedullary junction. In HK-2 cells, *Loganetin* could inhibit NF-κB pathway and pro-apoptotic genes expression. However, TLR4 was silenced by a specific shRNA, and the inhibitory effect of *Loganetin* in HK-2 cells vanished. *Loganetin* also down-regulated the expression of inflammation factors by suppressing TLR4 activity.

Conclusion and Implications: All the results suggested that TLR4 plays a critical role in AKI development, and *Loganetin* ameliorates AKI by inhibiting TLR4 activity and blocking the JNK/p38 pathway, which provides a new strategy for AKI treatment.

1 | INTRODUCTION

Acute kidney injury (AKI) is a rapid renal dysfunctional disease with severe tubular damage and is a global health problem, with more than 10 million people affected annually (Bellomo, Kellum, & Ronco, 2012). There are many causes of this disease, including ischaemic, obstructive, toxic, and infectious pathogens (Bellomo et al., 2012). One important cause of AKI is **sepsis** (Uchino et al., 2005). **LPS** plays an important role in the pathogenesis of sepsis-induced AKI (Xu et al., 2014). Therefore, LPS is used in models for experimental sepsis-induced AKI. AKI is a common complication and affects approximately 20% of hospitalized patients in both developed and developing countries (Mehta et al., 2016). Recently, it was reported that almost 2

Abbreviations: AKI, acute kidney injury; ATN, acute tubular necrosis; BUN, blood urea nitrogen; C-cas-3, cleaved caspase-3; CKD, chronic kidney disease; CREA, serum creatinine; PAS, periodic acid-Schiff; RIAKI, rhabdomyolysis-induced AKI; TLR4, Toll-like receptor 4

*To whom contributed equally to this study and share first authorship.

million people die of AKI every year, and the survivors have a high risk of chronic kidney disease (CKD; Li, Burdmann, & Mehta, 2013).

Although the pathophysiology of AKI is complex, we know that mitochondrial dynamics play important roles in AKI development. Mitochondrial dysfunction results in ROS generation, causing cellular damage via chemical modification of proteins, lipids, and nucleic acids (Valko, Jomova, Rhodes, Kuca, & Musilek, 2016). Patients with CKD or diabetes mellitus have increased steady-state levels of oxidative stress and are thus at high risk of developing AKI (Arora & Singh, 2014; Okamura & Pennathur, 2015). Therefore, oxidative stress has been implicated as one of the principal drivers of renal injury of AKI. It has been reported that increasing mitochondrial function can improve AKI (Jesinkey et al., 2014). Another characteristic of AKI is nephron loss via tubular epithelial cell programmed cell death triggering an immune response. Renal ischaemia is one of the major causes of AKI. An acute inflammatory process leads to cytokine and chemokine production (Kim et al., 2013). Both innate and adaptive immune cells are involved in renal ischaemic-induced AKI. During AKI, the expression of toll-like receptor 2 (**TLR2**) and **TLR4** are elevated in renal tubular epithelial cells (Jang, Ko, Wasowska, & Rabb, 2009).

TLRs, which belong to a superfamily of transmembrane receptors, recognize their respective ligands by molecular pattern recognition, which plays a key role in the innate immune system. Activation of TLRs induces the release of a series of cytokines and chemokines that attract inflammatory cells. TLR4, the receptor for endotoxin, is expressed on kidney microvascular endothelial cells and kidney tubular epithelial cells (El-Achkar et al., 2006; Wu et al., 2007). Importantly, it has been demonstrated that activation of TLR4 on both kidney microvascular endothelial cells and kidney tubular epithelial cells increases acute tubular injury and kidney dysfunction in ischaemic AKI (Chen et al., 2011; Pulskens et al., 2008; Wu et al., 2007; Wu et al., 2010). The function of TLR4 is involved not only in the acute phase of injury in kidney disease but also in regulating kidney fibrosis and CKD (Souza et al., 2015). Inhibition of TLR4 signalling relieves symptoms in mouse models of unilateral ureteral obstruction (Campbell et al., 2011).

Loganetin is a natural product from cornus fruits. It is well known that *Loganetin* can be obtained from *Loganin* enzymatically (Nagatoshi, Terasaka, Nagatsu, & Mizukami, 2011). Although the biological functions of *Loganetin* have been little investigated, the activities of *Loganin* have been studied extensively. *Loganin* can attenuate oxidative stress in SH-SY5Y cells by regulating **JNK**/**p38** and **ERK1/2** pathways (Kwon et al., 2011). It has also been shown that *Loganin* has neuroprotective effects in Parkinson's disease models (Yao et al., 2017). Recent studies have shown that *Loganin* inhibits inflammation and protects the kidney (Kim et al., 2015; Li et al., 2016; Liu et al., 2015; Zhao et al., 2016). However, whether *Loganetin* can modulate inflammation in AKI is not known.

There is currently no effective treatment for AKI. In the present study, we evaluated the effects of *Loganetin* on an AKI mouse model and explored its effects on TLR4 expression and the inflammation-associated NF-κB pathway. This research offers a new strategy for AKI treatment.

What is already known

- *Loganetin* is a natural small molecular product that has been shown to inhibit inflammation and protect the kidney from diabetic nephropathy.

What this study adds

- *Loganetin* displays anti-inflammatory and anti-apoptosis effects in the mouse kidney both in vitro and in vivo, and these are mediated by its suppression of the function of TLR4.

What is the clinical significance

- TLR4 has a critical role in the development of AKI and this study provides important data for the rational use of Loganetin for treating AKI in the clinic.

2 | METHODS

2.1 | Animals and rhabdomyolysis-induced AKI model

C57/BL6J mice (RRID:IMSR_JAX:000664, male, 6–8 weeks old, 18–22 g, n = 40) were purchased from Vital River Laboratory (Vital River Laboratory Animal Technology, Beijing, China). These mice were randomly divided into four groups, 10 mice per group. Thirty TLR4 knockout (TLR4-KO) mice C57BL/10ScNJ (RRID:IMSR_JAX:003752, male, 8 weeks old, 18–22 g) and 30 TLR4 wild-type (TLR4-WT) mice C57BL/10ScSn (RRID:IMSR_JAX:000476, male, 8 weeks old, 18–22 g) were obtained from the Model Animal Research Centre of Nanjing University (Nanjing, Jiangsu, China). Mice were randomly divided into three groups, 10 mice per group. All animals were housed in the centre for new drug safety evaluation of Lunan Pharmaceutical (Lunan Pharmaceutical Group Co., Ltd., Linyi, China) under a pathogen-free, temperature-controlled environment with a 12-hr light/dark cycle. The animals were supplied with pellet chow and water ad libitum. Mice were kept group-housed at five per cage in specific pathogen free (SPF) with corncob bedding. During the whole experiment, animal welfare was ensured. All experiments were in accordance with the experimental protocols previously approved by the Institute's Animal Ethics Committee at the Pharmacological centre of Lunan Pharmaceutical Group Co., Ltd., and were performed in accordance with the U.S. National Institutes of Health Guidelines for Care and Use of Laboratory Animals (National Research Council [U.S.] Committee for the Update of the Guide for the Care and Use of Laboratory Animals). Humane endpoints were deployed according to the report of Ashall and Millar (2014). Animal studies are reported in compliance with the ARRIVE guidelines (Kilkenny et al., 2010) and with the recommendations made by the *British Journal of Pharmacology*.

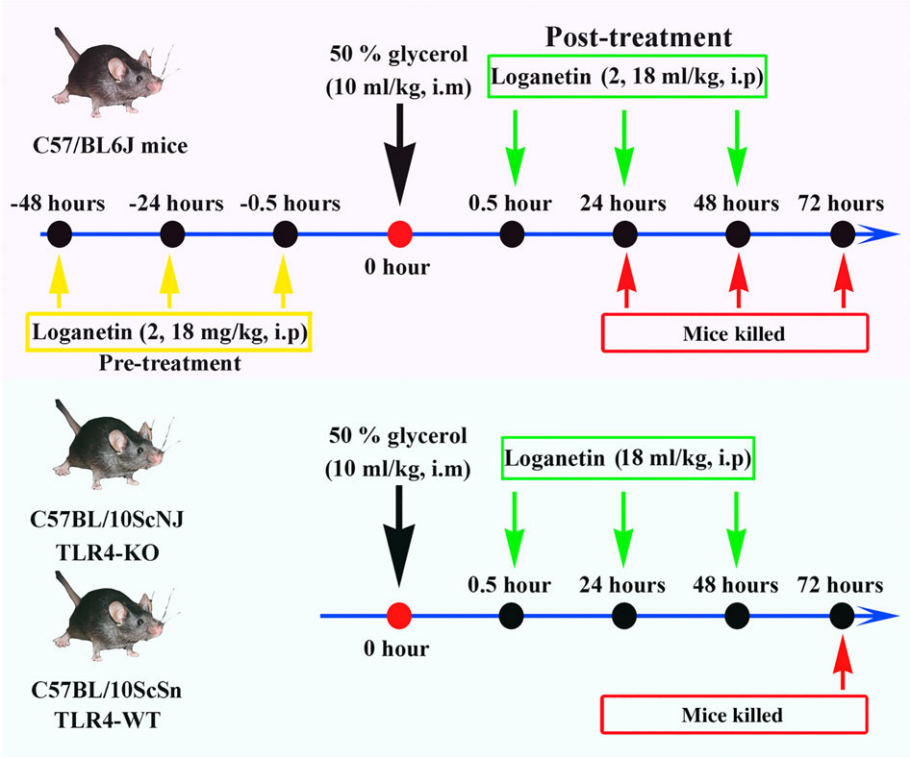

FIGURE 1 Experimental protocol for the induction of rhabdomyolysis-induced acute kidney injury in mice; 50% glycerol was administered i.m. into the hind limbs of mice at a dose of 10 ml·kg^{-1}. Saline-injected mice were used as controls. To determine the protective effect of *Loganetin*, 2 or 18 mg·kg^{-1} of body weight of *Loganetin* or PBS was administered i.p. at the indicated time points (0.5, 24, and 48 hr) post-acute kidney injury; 24, 48, and 72 hr after glycerol injection, mice were killed for blood and kidney samples

To achieve the rhabdomyolysis-induced AKI (RIAKI) model in mice, 50% glycerol was i.m. injected (10 ml·kg^{-1}) into the hind limbs of Balb/c mice. To investigate the possible protective effect of *Loganetin* against AKI, 40 mice were randomly divided into four groups, in the control (a) and model (b) groups, and 10 mice in each group underwent i.m. injected 50% glycerol or equal-volume saline respectively. In treatment group, 2 (c) or 18 mg·kg^{-1} (d) of *Loganetin* was administered i.p. 30 min and 24 and 48 hr after glycerol injection, and mice were anaesthetized using isoflurane (*Lunan* Pharmaceutical Group Co., Ltd., Linyi, Shan Dong Province, China) with an anaesthetic machine (model: SN-487, SHINANO MFG Co., Ltd., Japan) and killed at 24, 48, and 72 hr respectively. Blood and kidney tissues were collected for subsequent analysis. Finally, the animals were killed by abdominal aorta bleeding. The experimental protocol is summarized in Figure 1. To determine whether it is possible protective effects of *Loganetin* on the kidney occurred via TLR4, C57BL/10ScNJ (TLR4-KO, n = 30) and C57BL/10ScSn (TLR4-WT, n = 30) mice were administered saline as control group or 50% glycerol with or without *Loganetin* (18 mg·kg^{-1}) treatment, 10 mice per group, and samples were collected at 72 hr after glycerol injection.

2.2 | Renal function, histology, and TUNEL assay

To determine the kidney injury induced by glycerol and protective effects of *Loganetin*, serum creatinine (CREA) and blood urea nitrogen (BUN), indicators of kidney function, were evaluated using QuantiChrom Creatinine and UREA Assay Kits (BioAssay Systems, Hayward, CA) according to methods described previously (Press et al., 2017). To detect tissue injury, mice kidney tissues were fixed in 4% paraformaldehyde buffer for 24 hr and embedded in paraffin. Subsequently, paraffin blocks were cut into 2-μm sections and then subjected to routine H&E, PAS, and TUNEL staining according to previously described protocols (Wang, Li, et al., 2017; You et al., 2017; Zhang, Liu, et al., 2017). Histological differences among the groups were recorded. For H&E staining, five different fields from each group were randomly selected, and an acute tubular necrosis (ATN) score was used to indicate the tubular injury graded from 0 to 5 according to necrosis, dilation, and cast formation (0, none; 1, <15%; 2, 15% to 30%; 3, 31% to 50%; 4, 51% to 75%; 5, >75%). To quantify the PAS stain, the % area of brush border was calculated using image software. For TUNEL-stain semiquantitative analysis, 10 different fields from each group were randomly selected to count the TUNEL-positive cells·mm^{-1}.

2.3 | ELISA, immunohistochemistry, immunofluorescence, and immunoblot analysis

To determine the expression levels of inflammation factors (IFN-γ, TNF-α, IL-17A, IL-6, and IL-1β), mice sera were collected at different time points from each group and analysed by ELISA following methods from previous studies (Ren et al., 2016; Zhao et al., 2014). To investigate the levels of proteins in the TLR4-related signalling pathway, such as

TLR4, phospho-NF-κB p65 (p-p65) or nonphospho-NF-κB p65 (p65), JNK, p-JNK, p38, p-p38, p21, **c-Jun**, **Bax**, and cleaved **caspase-3**, kidney-paraffin blocks and tissues were subjected to immunohistochemistry, immunofluorescence, and immunoblot analysis. As in previous studies (Wang, Zhang, et al., 2017; Zhang, Wang, et al., 2017), the kidney-paraffin sections were rehydrated through a graded series of ethanol and then incubated in 0.3% **H_2O_2** overnight at 4°C to block endogenous peroxidase activity. Specific primary antibodies were incubated for 12 hr at 4°C in different dilutions (p-p65, p65, JNK, p38, 1:100; p-JNK, p-p38, p21, 1:150; c-Jun, Bax, cleaved caspase-3, 1:200). After DAB or fluorescence-conjugated antibody staining, five fields of the slides were collected from each animal at 20× and 40× magnification. For immunoblot assays, the procedures were based on previous studies (Li, Wan, et al., 2015; Li, Xie, et al., 2015). Briefly, kidney extracts were resuspended in a storage solution containing 100 mM Tris (pH 7.4), 0.1 mM EDTA, 0.1 mM dithiothreitol, 1.15% (w·v^{-1}) KCl, and 20% (v·v^{-1}) glycerol. To determine protein expression, the proteins (30 μg) were separated by SDS-PAGE. After transfer to PVDF membranes, samples were incubated overnight at 4°C with the respective antibodies at different dilutions (p-p65, p65, JNK, p38, 1:2000; p-JNK, p-p38, p21, 1:1500; c-Jun, Bax, cleaved caspase-3, 1:2500). All the blots were incubated with peroxidase-conjugated antibody (1:6000, Millipore, Billerica, MA) at room temperature for 1 hr. β-Actin (1:4000) was used as a loading control. The blots were visualized using chemiluminescence and imaged by the AutoChemi Imaging System (UVP LLC, Upland, CA). The blots were analysed using the MCID Elite software (InterFocus Imaging Ltd., Linton, UK). And the grey intensity of the phosphorylated protein was quantified and normalized to β-actin levels and expressed as phosphorylated protein/non-phosphorylated protein/β-actin. The immuno-related procedures used comply with the recommendations made by the *British Journal of Pharmacology*.

2.4 | Real-time PCR analysis

To evaluate mRNA expressions, total RNA was extracted from kidney tissues and cultured cells using the TRIzol reagent according to the manufacturer's protocol. cDNA was synthesized using a cDNA Synthesis Kit. All real-time PCR reactions with SYBR Green were performed and analysed with the ABI Prism 7500 instrument (Applied Biosystems, Foster City, CA). GAPDH was used for normalization of relative expression levels.

2.5 | Cell culture and treatments

Human renal proximal tubular epithelial (HK-2) cells were obtained from ATCC and maintained in DMEM/F12 medium containing 10% FBS. HEK293 cells stably expressing TLR4, **MD-2**, and CD14 were purchased from InvivoGen (HEK293-hTLR4/MD2-CD14, Catalog #293-htlr4md2cd14, RRID:CVCL_Y395, InvivoGen, San Diego, CA) and cultured in DMEM/F12 medium containing 10% FBS, blasticidin (10 μg·ml^{-1}), HygroGold (50 μg·ml^{-1}), and Normocin (100 μg·ml^{-1}).

Ice-cold RPMI 1640 medium was used to lavage the mice peritoneally to obtain macrophages, which were plated in 96-well plates at a density of 5 × 10^5 cells per well in RPMI complete medium.

Mice macrophages were pre-incubated with **TAK-242** (10 or 100 nM) or *Loganetin* (50, 100, or 200 nM) for 0, 15, 30, 45, 60, 75, or 90 min, and then the cells were washed and stimulated with 1 ng·ml^{-1} LPS or myoglobin (Sigma) for 6 hr. The expression levels of TNF-α and IL-6 in culture supernatants were determined by ELISA.

HEK293-hTLR4/MD2-CD14 cells were seeded in a 96-well plate at a density of 2 × 10^4 cells per well and cultured overnight. Cells were transfected with 10-ng phRL-TK as internal control and with 20-ng pNiFty or 30-ng pISRE-TA-Luc plasmid. At 6 hr after transfection, a series of graded concentrations of LPS, TAK-242, or *Loganetin* (from 10^{-4} to 10^6 nM) was added to the medium and incubated overnight. Subsequently, luciferase activities were determined by the Dual-Glo Luciferase Assay System. Experiments were performed in triplicate for each group, and the results are presented as mean + SD.

HK-2 cells (RRID:CVCL_0302) with or without shTLR4 plasmid transfection were pretreated with *Loganetin* (100 nM) for 0, 3, 6, 12, and 24 hr then washed and incubated with LPS (1 ng·ml^{-1}) for 6 hr. Then cells were fixed in 4% paraformaldehyde for immunofluorescence assays or lysed in cell lysis buffer for immunoblot assays.

In order to further identify the function of *Loganetin* in AKI, HK-2 cells or peritoneal macrophages were treated with 250 μM of myoglobin for 24 hr after *Loganetin* pretreatment. A TLR4-related signalling pathway in HK-2 cells was detected (Huang et al., 2018). And TNF-α and IL-6 levels in macrophages were determined by ELISA.

To thoroughly evaluate the effect of *Loganetin*, HK-2 cells were stimulated with LPS (1 ng·ml^{-1}) for 6 hr and then washed and incubated with *Loganetin* (100 nM) for 24 hr. Cell viability and apoptosis were determined.

2.6 | Flow cytometry and Annexin V/propidium iodide assay

Intact kidney tissues were decapsulated, diced, and digested in collagenase Type IV (ThermoFisher Scientific Inc. Waltham, MA) for 30 min at 37°C. The kidney tissue suspension was then passed through 40-μm Falcon meshes followed by red cell lysis. Single-cell suspensions were layered onto 34/51% discontinuous Percoll (GE Healthcare) density gradients and then centrifuged at 4,000× *g* for 30 min. Cells at the interface of the gradient were collected and washed twice with PBS. The cells were counted and incubated with anti-mouse CD3-APC, CD4-FITC, CD45-Per-CP, CD11b-PEcy5, F4/80-APC-Cy7, IFN-γ-PE or TNF-α-PE, and IL-17A-PE (Biolegend, San Diego, CA) for 1 hr at 4°C and detected on a BD Accuri C6 (BD Biosciences, San Jose, CA).

Cell death was analysed using the Annexin V-FITC/propidium iodide (PI) apoptosis detection kit (BD Biosciences, San Jose, CA). Briefly, cells were collected and washed with cold PBS twice and then resuspended in 1× binding buffer at a concentration of 1 × 10^6 cells·ml^{-1}. A 100 μl volume of this cell suspension was incubated with 5 μl Annexin V-FITC reagent and 5 μl PI reagent for 15 min. Binding buffer (400 μl) was added to each sample, and cells were analysed by flow cytometry. Annexin V−/PI− represents live cells; Annexin V+/PI− represents early apoptotic cells; Annexin V−/PI+ reflects necrosis; and double positivity indicates both late apoptosis and necrosis.

2.7 | Statistical analysis

Data are expressed as the mean ± SD. One-way ANOVA followed by Tukey's post hoc test was used to compare multiple treatment groups. Two-way ANOVA was used to assess the statistical significance of the differences between multiple treatment groups at different time points. Statistical significance was set at $P < 0.05$. The data and statistical analysis comply with the recommendations of the *British Journal of Pharmacology* on experimental design and analysis in pharmacology (Curtis et al., 2018).

2.8 | Chemicals, reagents, kits, and antibodies

High purity *Loganetin* (>99%) was obtained from the State Key Laboratory of Generic Manufacture Technology of Chinese Traditional Medicine (*Lunan* Pharmaceutical Group Co., Ltd., Linyi, Shan Dong Province, China). Glycerol (for molecular biology, >99%), LPS (#L2630), and myoglobin were purchased from Sigma (Sigma-Aldrich, St Louis, MO). **TAK-242** (#243984-11-4) and phalloidin-FITC conjugate were purchased from Millipore (MerckMillipore, Billerica, MA). SYBR Green was from Toyobo (Cat. K1621, TOYOBO, Osaka, Japan).

The TLR4 shRNA (h) and control shRNA plasmids were obtained from Santa Cruz Biotechnology (Santa Cruz, CA). TRIzol reagent was from Invitrogen (Carlsbad, CA), and the M-MLV reverse transcriptase was from Promega (Madison, WI). Ethanol and xylene (chromatographic grade) were purchased from Fisher Scientific Co. (Fisher Scientific, Houston, TX). Ultrapure HPLC-grade water was prepared using the Milli-Q® system.

Haematoxylin and eosin (H&E) stain kits (#C0105) and TUNEL kits (#C1098) were purchased from Beyotime Biotechnology (Beyotime Biotechnology, Shanghai, China). Periodic acid-Schiff (PAS) stain kits were obtained from Solarbio (#G1285, Solarbio Life Sciences, Beijing, China). Mouse IFN-γ, TNF-α, IL-17A, IL-6, and IL-1β ELISA kits were supplied by R&D Systems (Boston, MA). The ECL detection kit was from Thermo Scientific (#32106, Waltham, MA), the cDNA Synthesis Kit was from TOYOBO (Osaka, Japan), and the Dual-Glo Luciferase Assay System was purchased from Promega (#E2920, Madison, WI).

TLR4 rabbit mAb (#14358), NF-κB p65 rabbit mAb (#8242, RRID:AB_10859369), phospho-NF-κB p65 (Ser^{536}) rabbit mAb (#3033, RRID:AB_331284), JNK rabbit mAb (#9252, RRID:AB_2250373), phospho-JNK (Thr^{183}/Tyr^{185}) rabbit mAb (#4668, RRID:AB_823588), p38 rabbit mAb (#2387, RRID:AB_11178801), Phosphor-p38 (Thr^{180}/Tyr^{182}) rabbit mAb (#4511, RRID:AB_2139682), p21 rabbit mAb (#2947, RRID:AB_823586), c-Jun rabbit mAb (#9165, RRID:AB_2130165), Bax rabbit mAb (#14796, RRID:AB_2716251), cleaved caspase-3 (C-cas-3; Asp^{175}) rabbit mAb (#9664, RRID:AB_2070042), and β-actin mouse mAb (#3700, RRID:AB_2242334) were purchased from CST (Cell Signaling Technology, Boston, MA).

2.9 | Nomenclature of targets and ligands

Key protein targets and ligands in this article are hyperlinked to corresponding entries in http://www.guidetopharmacology.org, the common portal for data from the IUPHAR/BPS Guide to PHARMACOLOGY (Harding et al., 2018), and are permanently archived in the Concise Guide to PHARMACOLOGY 2017/18 (Alexander, Fabbro et al., 2017a,b; Alexander, Kelly et al., 2017).

3 | RESULTS

3.1 | *Loganetin* protected against rhabdomyolysis-induced kidney injury in mice

Initially, we investigated and confirmed the protective effects of *Loganetin* against RIAKI in C57/BL6J mice. The protocols are summarized in Figure 1. *Loganetin* (2 or 18 $mg{\cdot}kg^{-1}$) was i.p. injected 0.5, 24, and 48 hr after 50% glycerol injection. Mice were killed at 24, 48, and 72 hr, and kidneys and blood were collected for the following experiments.

As shown in Figure 2, kidney H&E staining demonstrated that glycerol injection induced significant kidney tissue damage in C57/BL6J mice, especially in the kidney tubular structures. This damage was significantly ameliorated in *Loganetin*-treated mice in both 2 and 18 $mg{\cdot}kg^{-1}$ treatment groups. The injury (glycerol-induced) and protection (*Loganetin*-mediated) were time- and dose-dependent (Figure 2a). The hind limb muscle tissues of mice from each group were collected, and H&E staining results showed that neither 2 nor 18 $mg{\cdot}kg^{-1}$ *Loganetin* ameliorated the degree of rhabdomyolysis compared with glycerol + PBS (Figure 2b). To quantitfy tubular injury, ATN scores of 72-hr-treated mice were calculated according to a series evaluation standard that included tubular necrosis, tubular dilation, and cast formation (Figure 2c). Glycerol treatment resulted in dramatically more damage (ATN score 4.0 ± 1.0) compared with the control group, but this damage is significantly less with *Loganetin* treatment at both dosages (2 $mg{\cdot}kg^{-1}$, 2.9 ± 0.5; 18 $mg{\cdot}kg^{-1}$, 1.5 ± 0.5). The survival status in each group (n = 10 in each group) were recorded by electronic monitoring equipment, and survival rates were calculated using GraphPad Prism 5 software (GraphPad Software, La Jolla, CA; Figure 2d). There were no mice in the control group that died throughout the course of the experiment (72 hr). However, a 50% (n = 5) mortality rate was observed in the glycerol-treated group, and these deaths occurred in the early stage (from the 30th to 65th hour). In contrast, *Loganetin* treatment resulted in a lower mortality rate at both 2- and 18-$mg{\cdot}kg^{-1}$ dosages (30% and 10%, respectively) and lower death incidence at the end of this study (from the 58th to 66th hour). Meanwhile, the long-term protective effects of *Loganetin* on mortality were evaluated when mice were pre or post-treated with *Loganetin* and using the following procedure. Mice received an i.p. injection for three consecutive days. After the last injection, 50% glycerol was i.m. injected (10 $ml{\cdot}kg^{-1}$) into the hind limbs of mice, and the mortality rates were recorded for 15 days. The results are shown in Supporting Information Figure S1g; no death occurred in the control group. Compared with the control group, a 90% mortality rate (n = 9) in glycerol-treated group occurred during the early stage (from the second to the fifth day). Post-treatment with *Loganetin* significantly reduced the mortality compared with the model group such that the mortality rates were 70%

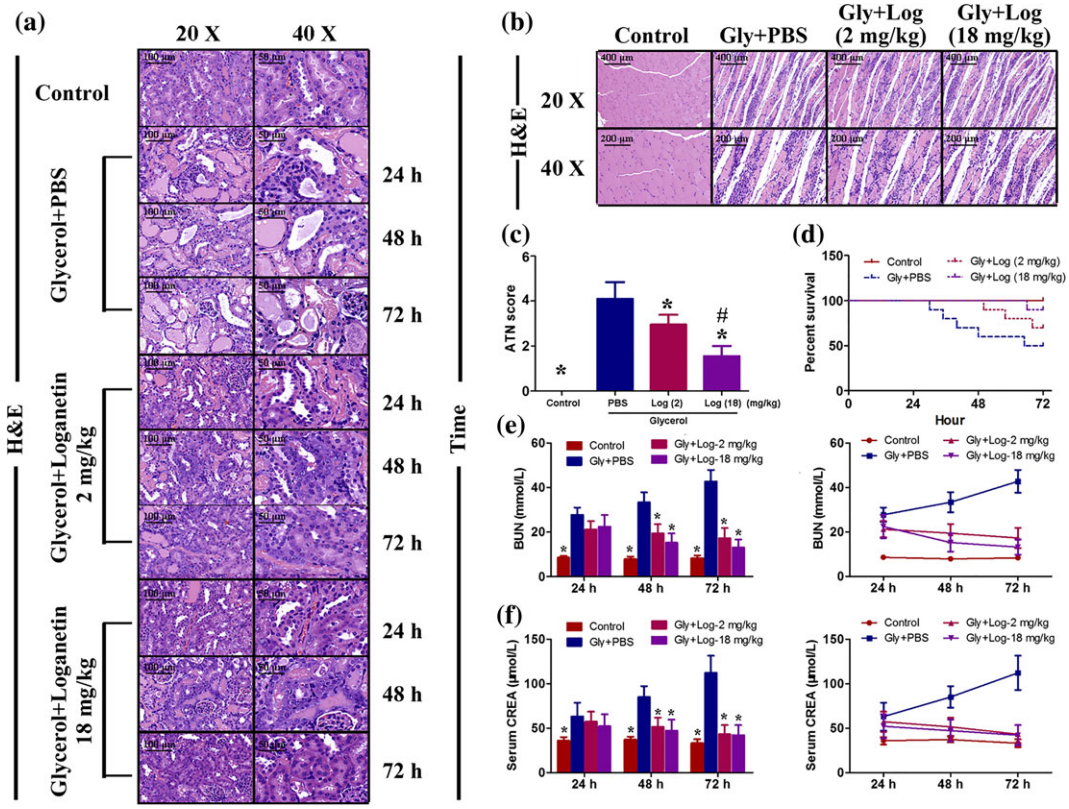

FIGURE 2 *Loganetin* ameliorated renal dysfunctions in rhabdomyolysis-induced acute kidney injury. Mice subjected to different treatments were killed at the indicated time points. Representative haematoxylin and eosin staining images of kidney (a) and muscle (b) tissue in each group are shown, and the acute tubular necrosis scores at 72 hr (c) were calculated. (d) Representative survival curves of each group. Serum levels of (e) creatinine (CREA) and (f) blood urea nitrogen (BUN) were measured, and the results are presented as bars (left) and curves (right). Bar = 100 μm. Data are expressed as the means ± SD, n = 10. *P < 0.05 versus Gly + PBS group; #P < 0.05 versus *Loganetin* 2 mg·kg^{-1} group

and 50% in 2- and 18-mg·kg^{-1} treatment respectively. Furthermore, it is noticeable that pre-*Loganetin* treatment exhibited a more efficient protective effect, further reducing the mortality rates (50% and 30% in *Loganetin* 2- and 18 mg·kg^{-1}, respectively) and prolonging the life span. In the 2 mg·kg^{-1} *Loganetin* pretreated group, three deaths occurred in the early stage (two in Day 3 and one in Day 5), and two in the end-stage (one in Day 9 and one in Day 11) of this study. In contrast, one animal died in the early (Day 4), mid- (Day 8), and end-stage (Day 12) in the 18 mg·kg^{-1} *Loganetin* pretreatment group respectively. In addition, BUN and serum CREA, which are biomarkers for kidney function, were evaluated using respective kits. The results showed that, compared with control mice, the glycerol injection caused obvious increases in serum CREA and BUN. In contrast, treatment with *Loganetin* significantly improved kidney function (Figure 2e,f). Subsequently, to precisely evaluate the tubular changes after glycerol with or without *Loganetin* administration, PAS staining was performed to clearly show intratubular cast and brush border loss. As shown in Figure 3a, glycerol caused significant damage to the tubular structure, characterized by swelling and degeneration of the tubular epithelial cells, disappearance of the brush border, necrosis of part of the epithelial cells, and formation of myoglobin tubes. *Loganetin* inhibited this pathological process in a dose-dependent manner; *Loganetin* treatment preserved the brush borders and reduced the occurrence of intraluminal casts (Figure 3a). To further evaluate apoptosis in kidney tissues during RIAKI, TUNEL staining was performed, and the results showed that there were significantly more apoptotic cells at the corticomedullary junction in mice subjected to glycerol injection. Consistent with kidney function and morphology, administration of *Loganetin* at both dosages suppressed this apoptosis markedly (Figure 3b). Semiquantitative analyses of PAS and TUNEL assays are presented in Figure 3c,d respectively.

To further investigate the role of *Loganetin* alone on kidney function, 2 or 18 mg·kg^{-1} of *Loganetin* were injected i.p. 0.5, 24, and 48 hr after saline injection. H&E, PAS, and TUNEL staining were performed after 72 hr. Compared with the control group, both the 2 and 18 mg·kg^{-1} *Loganetin* groups showed a potential trend but no significant effects on the kidney function and morphology including tubular injury (ATN score), kidney function (BUN and CREA), brush border, and TUNEL-positive cells (Supporting Information Figure S1a–f).

3.2 | The TLR4/JNK/p38 pathway was involved in the protective effects of *Loganetin*

To investigate the factors probably involved in the protective role of *Loganetin* in RIAKI mice, protein levels of the kidney tissues of each group were analysed by immunohistochemistry (IHC) staining. As shown in Figure 3e, phospho-p65, -JNK, -p38, p21, c-Jun, Bax,

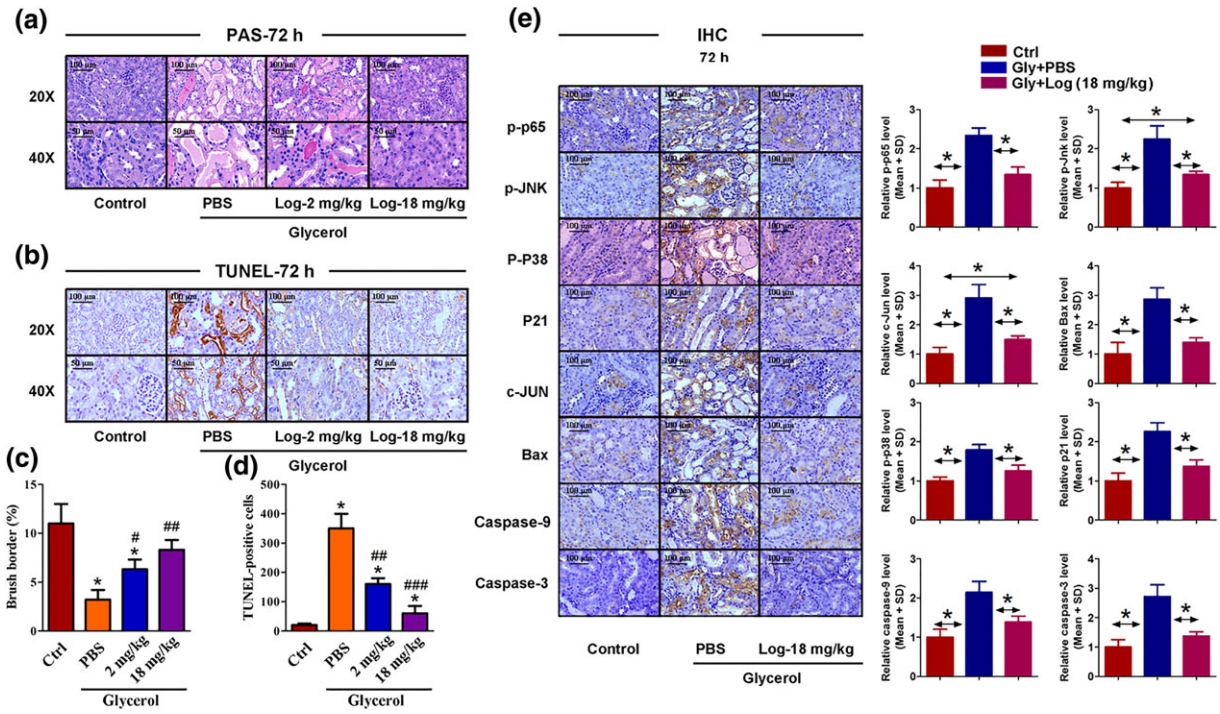

FIGURE 3 *Loganetin* inhibited apoptosis of tubular epithelial cells and regulated TLR4-related protein expression in rhabdomyolysis-induced acute kidney injury. Representative images of periodic acid-Schiff staining (a) and TUNEL staining (b) and respective semi-quantification of brush borders (c) and TUNEL-positive cells (d). Representative images of immunohistochemistry assays of kidney tissues with p65, JNK, p38, and phospho-p65, -JNK, -p38, p21, c-Jun, Bax, caspase-9, and cleaved caspase-3 (e). Bar = 100 μm. Data are expressed as the means ± SD, $n = 10$. $^*P < 0.05$ versus Gly + PBS group; $\#P < 0.05$ versus *Loganetin* 2 mg·kg^{-1} group

caspase-9, and C-cas-3 were increased in the glycerol injection group compared with the control group. *Loganetin* showed an inhibitory effect on the expression of these proteins (Figure 3e, left). IHC staining was quantified by Panoramic Scan (3DHISTECH Ltd., Budapest, Hungary) and calculated by Caseviewer Software (QuantCenter version, 2.0.0.61665, 3DHISTECH Ltd., Budapest, Hungary), and the results are shown in Figure 3e (right). To further confirm these differences in protein levels, proteins were extracted from the kidney tissues of each group, and the relative expression levels were evaluated by immunoblot (Figure 4a,b). These results were consistent with the IHC staining. The relative mRNA expression levels in mouse kidney tissues were detected by qRT-PCR, and the primer sequences and results are shown in Supporting Information Figure S2.

3.3 | *Loganetin* ameliorated RIAKI-associated renal inflammation

Flow cytometry was performed to evaluate the inflammatory state by detecting cytokines in kidney tissues. The levels of pro-inflammatory cytokines, including IFN-γ, TNF-α, and IL-17A (Figure 5a–f), and inflammatory cells including CD3+ T cells, CD45+ immune cells, and CD11b + F4/80+ macrophages (Figure 5 l–n) were all significantly higher in mice injected with glycerol compared to the control mice. *Loganetin* treatment partially reduced this increase (Figure 5a–i). Similar consequences were observed for IL-6, IL-1β, TNF-α, IFN-γ, and IL-17A in mouse serum by ELISA assays (Figure 5g–k). However, TNF-α and IL-6 concentrations in peritoneal macrophages stimulated with myoglobin were significantly decreased after *Loganetin* treatment (Supporting Information Figure S3). Relative mRNA levels were determined by qRT-PCR, and the primer sequences and results are shown in Supporting Information Figure S4. All these results were consistent with kidney function and histological results and indicated that *Loganetin* has the ability to act as a potential immunomodulator.

3.4 | *Loganetin* is a TLR4 antagonist and blocked JNK/p38 pathway in vitro

Loganetin is known to inhibit pro-inflammatory factors and multiple molecules involved in the TLR4 signal pathway. Based on these clues, we hypothesize that this chemical modulates the activity of TLR4. To explore this hypothesis, NF-κB and ISRE Luciferase-report plasmids (pNiFty and pISRE-TA-Luc) were used to transfect HEK293-hTLR4/MD2-CD14 cells, which were subsequently stimulated by LPS with or without *Loganetin* or TAK-242 pretreatment. The results demonstrated that LPS, the classic TLR4 ligand, dramatically induced the activity of both pNiFty and pISRE-TA-Luc plasmids at extremely low concentrations (EC_{50} were 6.09 ± 1.13 and 6.41 ± 1.45 nM, respectively). In contrast, TAK-242 and *Loganetin* treatment resulted in lower pNiFty (IC_{50} of TAK-242, 8.08 ± 1.23 nM; IC_{50} of *Loganetin*,

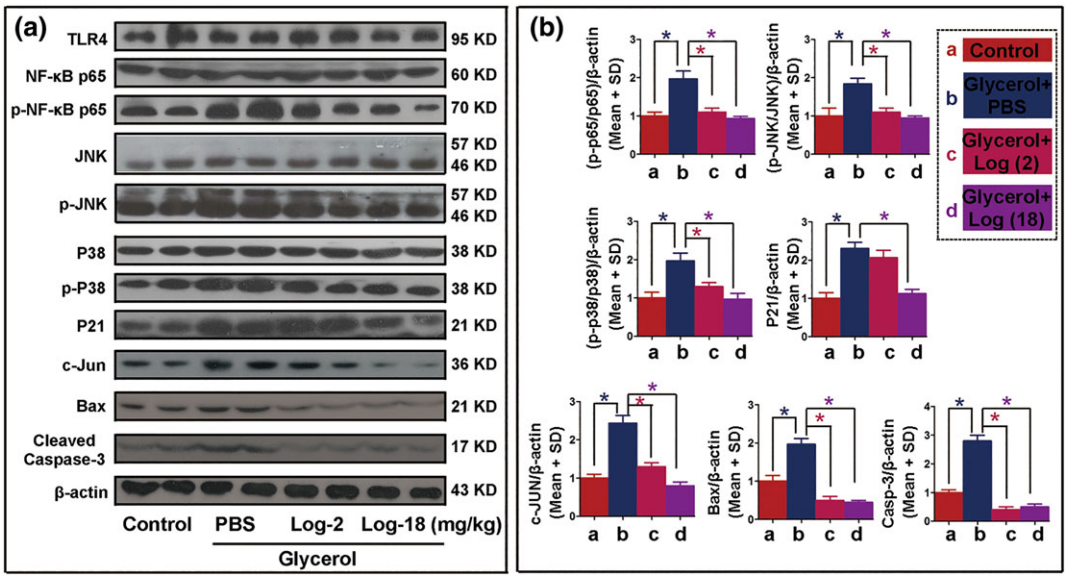

FIGURE 4 *Loganetin* regulated the protein expressions of TLR4/JNK/p38 pathway in rhabdomyolysis-induced acute kidney injury. Seventy-two hours after glycerol or saline injection, kidney tissue proteins were extracted from the control group and rhabdomyolysis-induced acute kidney injury mice with or without *Loganetin* treatment. The samples were analysed for TLR4, p65, p-p65, JNK, p-JNK, p38, p-p38, p21, c-Jun, Bax, cleaved caspase 3, and β-actin using specific antibodies. (a) Representative immunoblot analysis. (b) Immunoblot signals were quantified by densitometry and normalized with β-actin. The (p-p65/p65)/β-actin, (p-JNK/JNK)/β-actin, (p-p38/p38)/β-actin, p21/β-actin, C-Jun/β-actin, BAX/β-actin, and cleaved caspase 3/β-actin ratios are shown. Shown are representative blots and expressed as the means ± SD from series with tissues from n = 10; the bars with different superscripts in each panel were significantly different. $^{*}P < 0.05$ versus Gly + PBS group

25.4 ± 3.12 nM) and pISRE-TA-Luc (IC_{50} of TAK-242, 3.09 ± 0.53 nM; IC_{50} of *Loganetin*, 4.75 ± 0.76 nM) activity (Figure 6a,b). In addition, mouse peritoneal macrophages were lavaged from each group, cultured and pre-incubated with TAK-242 or *Loganetin* in a concentration series for different times, and then stimulated with LPS. TNF-α and IL-6 were detected by ELISA. Pre-treatment with *Loganetin* (200 nM) for 60 min showed significant inhibitory effects on the production of TNF-α and IL-6 (Figure 6c,d). Even at lower concentrations (100 or 50 nM), longer pre-incubations increased the inhibitory efficacy.

To determine the time course of the inhibitory effect of *Loganetin* on the production of TLR4-related proteins in vitro, HK-2 cells were incubated with *Loganetin* (100 nM) from 0 to 24 hr and then replaced by LPS. A total of 11 proteins were detected by immunoblot and are shown in Figure 6e. LPS (1 ng·ml^{-1}) significantly elevated the expression of seven proteins (p-p65, p-JNK, p-p38, P21, c-Jun, Bax, and C-cas-3). *Loganetin* exhibited rapid inhibitory effects on p-p65, p-p38, p-JNK, and C-cas-3 expression as early as 3 hr, followed by a subsequent decrease in inhibition thereafter (Figure 6e). However, non-phosphorylated proteins, such as p65, JNK, p38, and even TLR4, were not affected by either LPS or *Loganetin*. All semiquantitative results are shown in Figure 6f,g. Relative mRNA levels were determined by qRT-PCR and are shown in Supporting Information Figure S5.

In contrast, to verify the protective effects of *Loganetin*, HK-2 cells were post-treated with *Loganetin* (100 nM) for 24 hr after LPS (1 ng·ml^{-1}) stimulation (6 hr). From the results shown in Supporting Information Figure S6, compared with the LPS-treated group, *Loganetin* significantly reduced cell apoptosis rate and enhanced cell viability in a time-dependent manner.

To further confirm that TLR4 could mediate the protective effects of *Loganetin*, the shTLR4 plasmid was used to transfect HK-2 cells, and then immunoblot and immunofluorescence assays were used to compare related proteins expression with TLR4-WT HK-2 cells after both cell lines had been pretreated with or without *Loganetin* for 12 hr during LPS stimulation. Immunoblot and immunofluorescence assays demonstrated that TLR4 was almost completely inhibited by the shTLR4 plasmid (Figure 7a). Compared with the control, TLR4-KO showed significantly lower p-p65, p-JNK, p-p38, p21, c-Jun, Bax, and C-cas-3 expression. These protein levels were higher in TLR4-WT cells stimulated with LPS but lower with *Loganetin* pre-incubation for 12 hr. However, in TLR4-KO cells, no inhibitory effects of *Loganetin* on protein expression were observed, which indicates that TLR4 mediated *Loganetin's* effects on protein levels (Figure 7b). The results of a semiquantitative analysis are presented. To clearly demonstrate these mechanisms, immunofluorescence assays with p-JNK, p-p38, p21, and c-Jun antibodies were performed, and the results were consistent with those of the immunoblot assays (Figure 7c–f). Relative immunofluorescence values are shown in Supporting Information Figure S7.

3.5 | *Loganetin* inhibited the apoptosis of tubular epithelial cells in response to LPS

Although necrosis of epithelial cells has long served as an important indicator of AKI, one group has reported that this feature is more

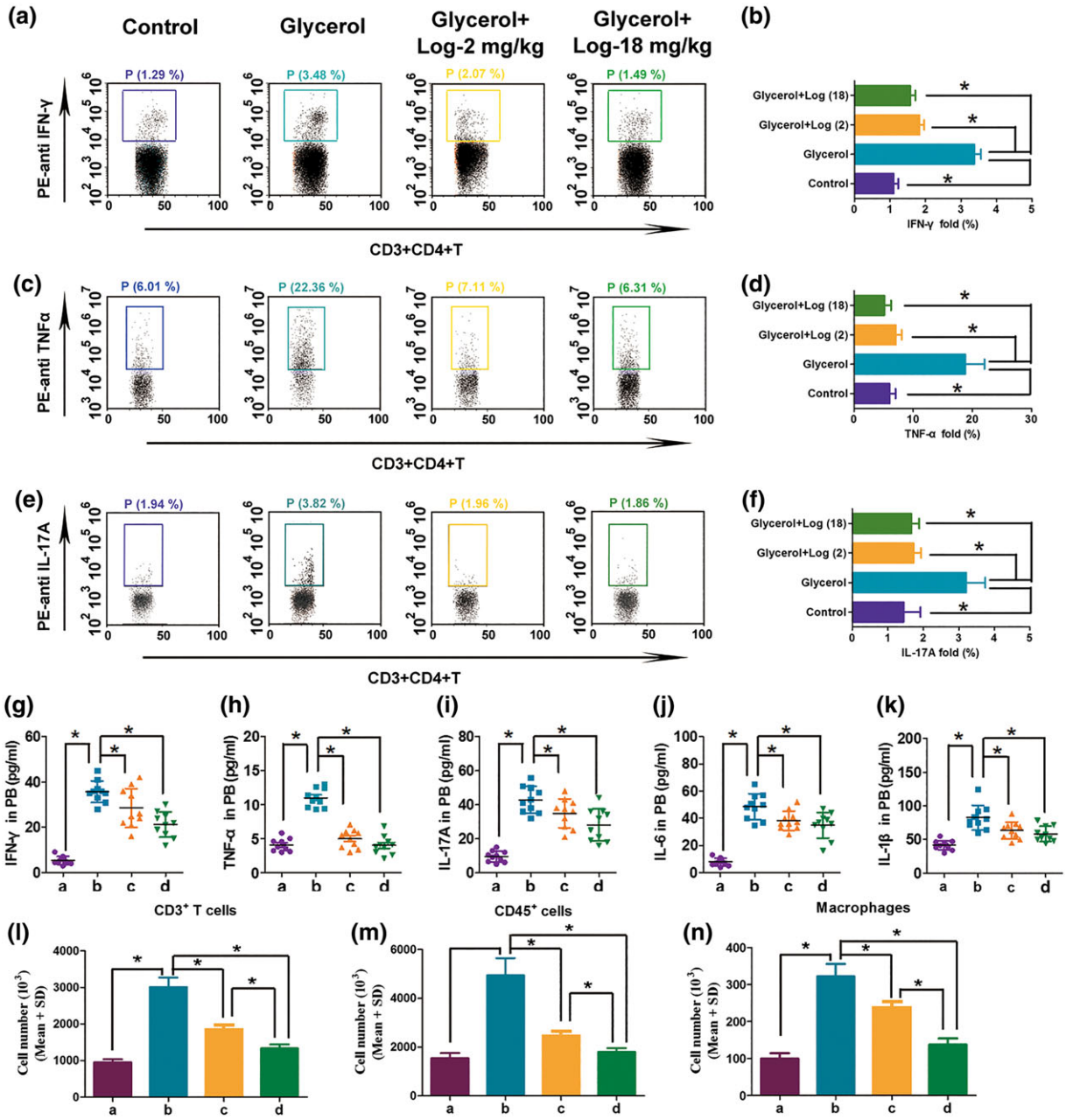

FIGURE 5 *Loganetin* ameliorated inflammation in rhabdomyolysis-induced acute kidney injury mice. (a,b) IFN-γ, (c,d) TNF-α, and (e,f) IL-17A were assayed by Flow cytometry. (g–k) IFN-γ, TNF-α, IL-17A, IL-6 and IL-1β in peripheral blood were analysed by ELISA. (l–n) CD3 + T cells, CD45+ immune cells, and CD11b + F4/80+ macrophages in kidney tissue were detected by Flow cytometry. Data are expressed as the means ± SD, $n = 10$. $^*P < 0.05$

suitable for the pathognomonic lesions of ischaemic AKI (Press et al., 2017). Thereafter, researchers have found that apoptosis plays a crucial role in the pathogenesis of AKI, which even outweighs necrosis (Wang, Li, et al., 2017; Zhang, Liu, et al., 2017; Zhao et al., 2014). Therefore, we explored whether *Loganetin* was involved in modulating apoptosis of kidney epithelial cells in RIAKI. First, the effects of *Loganetin* on HK-2 cell apoptosis and viability were tested by morphology and MTT assays respectively. In TLR4-WT cells, *Loganetin* pretreatment ameliorated LPS-induced tubular cell apoptosis (from 18.5 ± 3.2% to 9.46 ± 2.14%) and reductions in viability (Figure 8a,b; from 41.3 ± 9.6% to 87.4.3 ± 11.3%). However, when TLR4 was depleted by the shTLR4 plasmid, neither single LPS treatment nor LPS combined with *Loganetin* had any effect on apoptosis and viability (Figure 8a,b), which confirmed that *Loganetin* could inhibit apoptosis, and this activity was mediated by TLR4. Subsequently, flow cytometry analysis based on Annexin V/PI (AV/PI) staining was performed to detect different types of cell death. The staining results can be divided into four quadrants: AV−/PI− and AV+/PI+ represent live and late apoptosis plus necroptosis cells, respectively, and AV+/PI− and AV−/PI+ reflect early apoptosis and necroptosis cells respectively. Consistent with previous

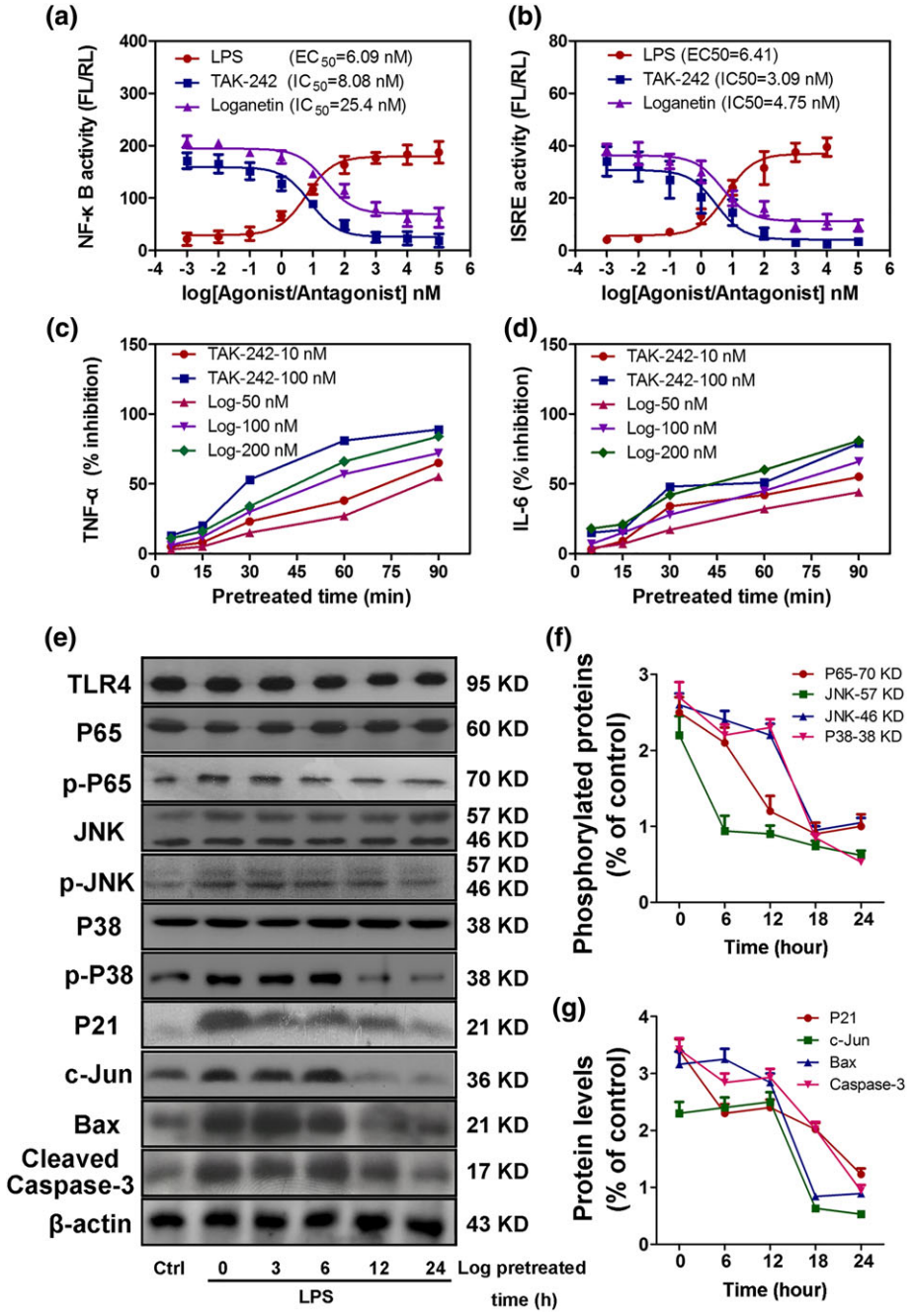

FIGURE 6 *Loganetin* is a potential TLR4 antagonist and regulates TLR4-related protein expression in vitro. The inhibitory effects of *Loganetin* on NF-κB and ISRE activation in HEK293-hTLR4/MD2-CE14 cells (a,b). Cells were transfected with 10-ng phRL-TK as an internal control, and 20-ng pNiFty (a) or 30-ng pISRE-TA-Luc (b) plasmid. Six hours after transfection, a series of graded LPS, TAK-242, or *Loganetin* concentrations (from 10^{-4} to 10^{6} nM) was added to the medium and treated overnight. Subsequently, luciferase activities were determined. Time- and concentration-dependence of the inhibitory effect of *Loganetin* on the production of TNF-α and IL-6 in mouse peritoneal macrophages stimulated with LPS were determined. Cells were incubated with TAK-242 or *Loganetin* at the indicated times, washed, and stimulated with LPS. The concentrations of TNF-α (c) and IL-6 (d) in the culture supernatants were determined using specific ELISA kits. (e–g) HK-2 cells pretreated with *Loganetin* (100 nM) at the indicated times, washed, and stimulated with LPS (1 ng·ml^{-1}) for 6 hr were lysed using cell lysis buffer for immunoblots. Experiments were performed in triplicate for each group

results, exposure to LPS caused a significant decrease in cell viability, especially in early apoptosis of cells, compared to vehicle-treated TLR4-WT-HK-2 cells. Moreover, addition of *Loganetin* obviously reduced early apoptosis rates. However, in TLR4-KO-HK-2 cells, LPS and *Loganetin* did not influence cell apoptosis rates. Compared with WT-HK-2 cells, TLR4 depletion reduced LPS-induced pro-apoptosis and *Loganetin*-mediated anti-apoptotic effects (Figure 8c). The relative quantitative analyses are presented in Supporting Information Figure S8a. Overall, these data suggested that *Loganetin* could suppress apoptosis of tubular epithelial cells, which is mediated by TLR4.

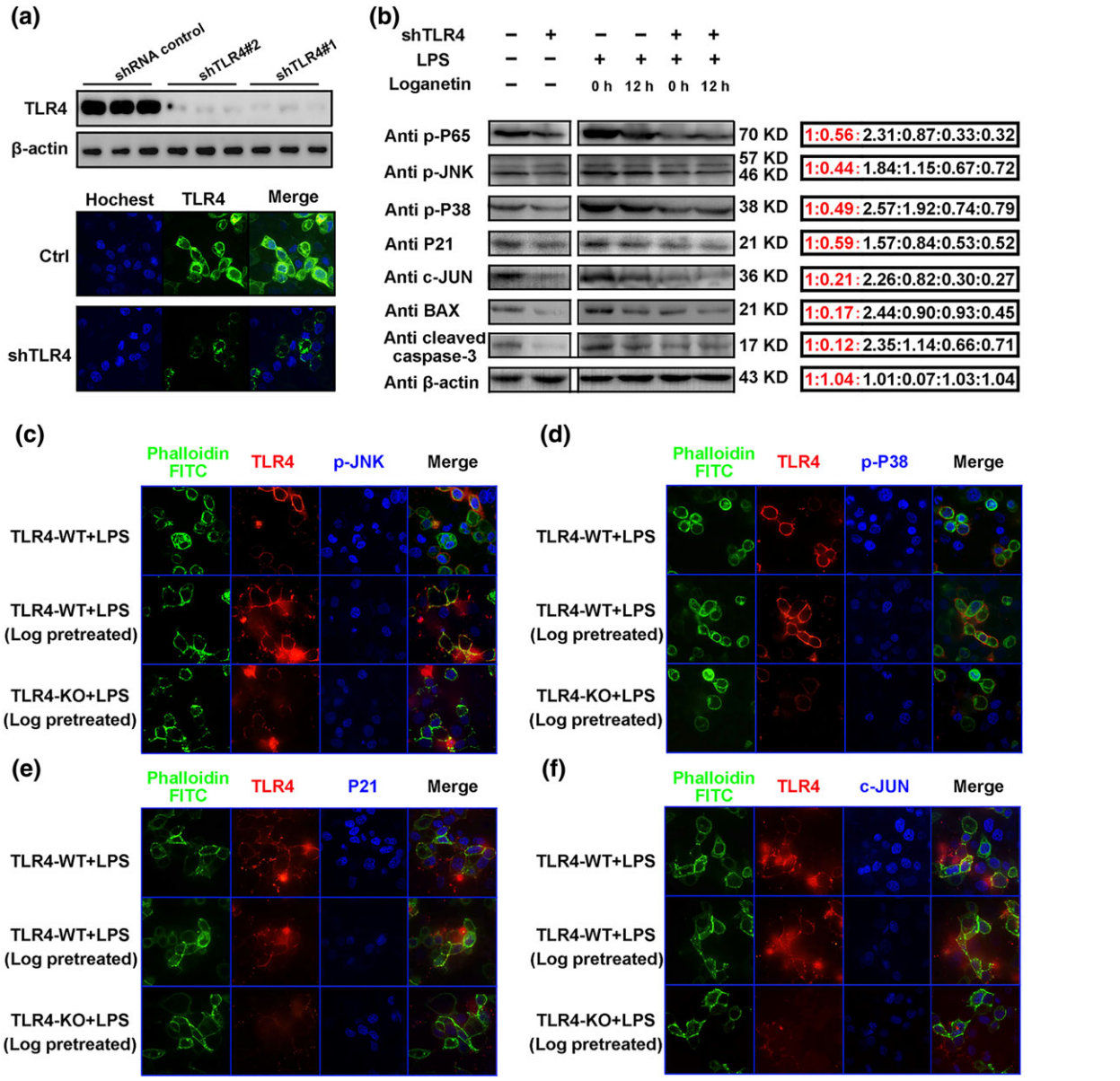

FIGURE 7 The protective mechanisms of *Loganetin* on HK-2 cells were mediated by the TLR4. TLR4 expression in HK-2 cells transfected with shTLR4 plasmid was determined by Western blot and immunofluorescence (a). HK-2 cells with or without shTLR4 plasmid transfection were pretreated with *Loganetin* (100 nM) for 0 and 12 hr, then washed and incubated with LPS (1 ng·ml^{-1}) for 6 hr, and lysed in cell lysis buffer for immunoblots (b) or fixed in 4% paraformaldehyde for immunofluorescence assays (c–f) respectively. Experiments were performed in triplicate for each group

3.6 | Deletion of TLR4 ameliorated renal dysfunction, renal injury, apoptosis, and cell death in RIAKI mice

To further clarify whether *Loganetin* exerts its protective effects on renal damage via TLR4, C57BL/10ScSn mice were treated with glycerol (50%, 10 ml·kg^{-1}, i.m. injection) alone or combined with LPS (1 mg·kg^{-1}, i.p. injection) with or without *Loganetin* (18 mg·kg^{-1}, i.p. injection). After 72 hr, all mice were killed, and the kidney function and morphology including ATN score, brush border, and TUNEL-positive cells were evaluated. The histological results demonstrated that glycerol-induced renal damage was enhanced when glycerol was combined with LPS injection but significantly ameliorated by *Loganetin* treatment. In addition, compared with glycerol only group, the protective effect of *Loganetin* on renal damage in the glycerol + LPS group was weaker but not significant (Supporting Information Figure S9a). In addition, PAS and TUNEL staining were performed, and relative parameters such as ATN score, brush border, and TUNEL-positive cells (Supporting Information Figure S9b) were in accordance with the H&E staining.

To further confirm previous results and our hypothesis, TLR4 knockout (TLR4-KO) mice were used to duplicate an RIAKI mouse model. Based on the immunoblot and qRT-PCR analysis, TLR4 was completely abolished in TLR4-KO mice compared with WT mice, even

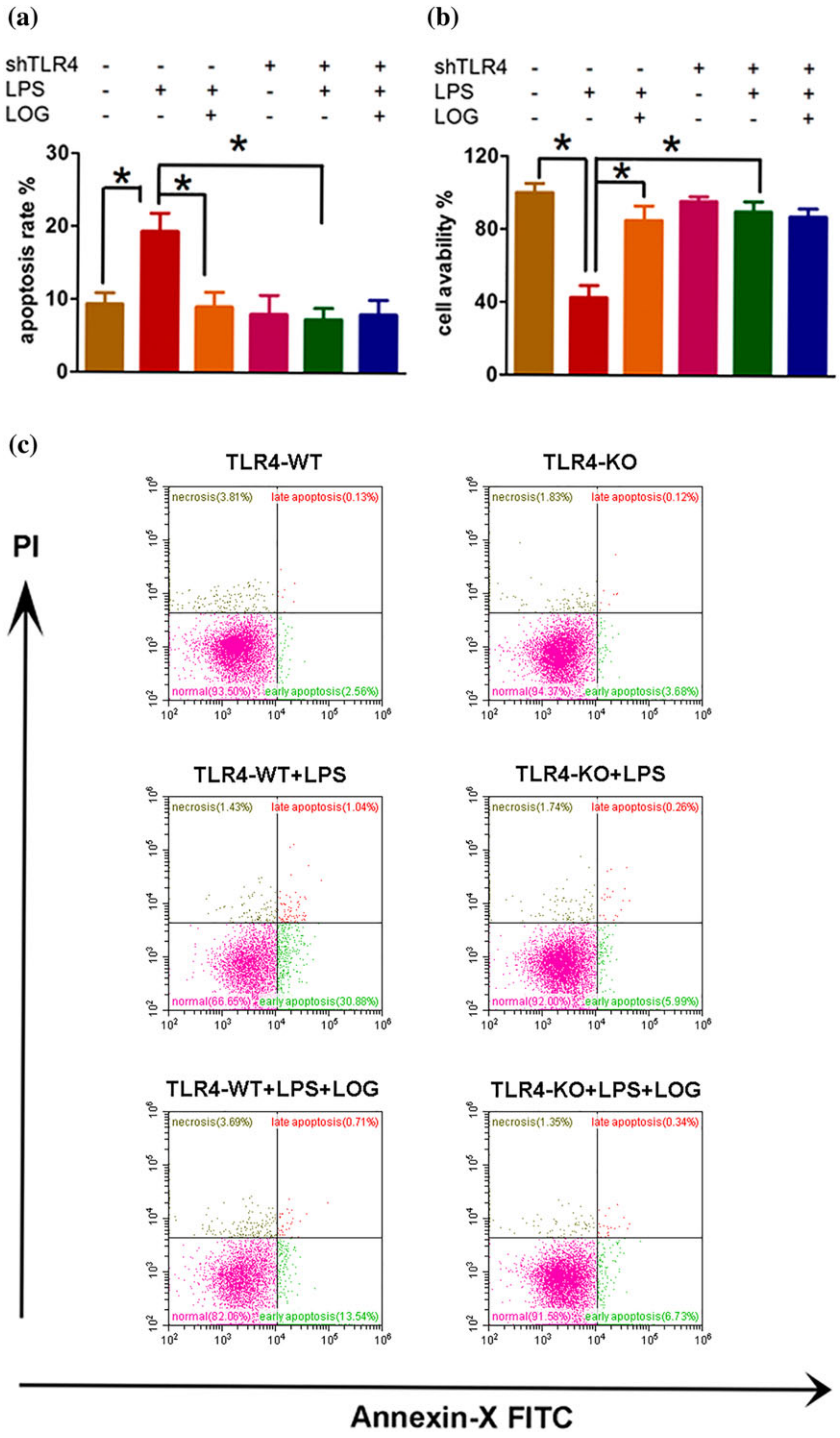

FIGURE 8 Deletion of TLR4 ameliorated renal dysfunction, renal injury, apoptosis, and cell death in vivo and in vitro. The anti-apoptotic effects of *Loganetin* on HK-2 cells were compared with or without shTLR4 plasmid transfection; apoptosis rate (a) and cell viability (b) were determined. To explore the role of *Loganetin* in LPS-induced cell death, cells were collected and analysed by flow cytometry based on Annexin V/PI staining (c). Experiments were performed in triplicate for each group. Data are expressed as the means ± SD. $^*P < 0.05$

after glycerol treatment (Supporting Information Figure S7). To assess the role of TLR4 in the pathogenesis of RIAKI, wild-type and TLR4-KO littermate mice were treated with or without *Loganetin* (18 mg·kg^{-1}) for 72 hr after glycerol injection. The survival status of all treatment groups was recorded and calculated (Figure 9b). Compared with the control group (none died), mortality was higher both in the WT (five died between the 36th and 59th hour after glycerol injection) and KO mice (two died between the 40th and 69th hour after glycerol injection) treated with glycerol. In contrast, *Loganetin* treatment resulted in dramatically lower mortality in both TLR4-WT-RIAKI mice (three died) and TLR4-KO-RIAKI mice (two died). In addition to the elevated survival percentage, *Loganetin* prolonged lifespan regardless of whether TLR4 was knocked out. In the non-*Loganetin* treatment group, levels of BUN and serum CREA were similarly low. At 72 hr after glycerol injection, wild-type mice developed moderate renal failure, which was significantly lower with *Loganetin* treatment or in TLR4-KO mice without *Loganetin* treatment. However, the levels of BUN and CREA were not different between WT or KO mice after *Loganetin* treatment (Figure 9b). Histological analysis confirmed that the glycerol-induced kidney tissue damage occurred in TLR4-WT mice,

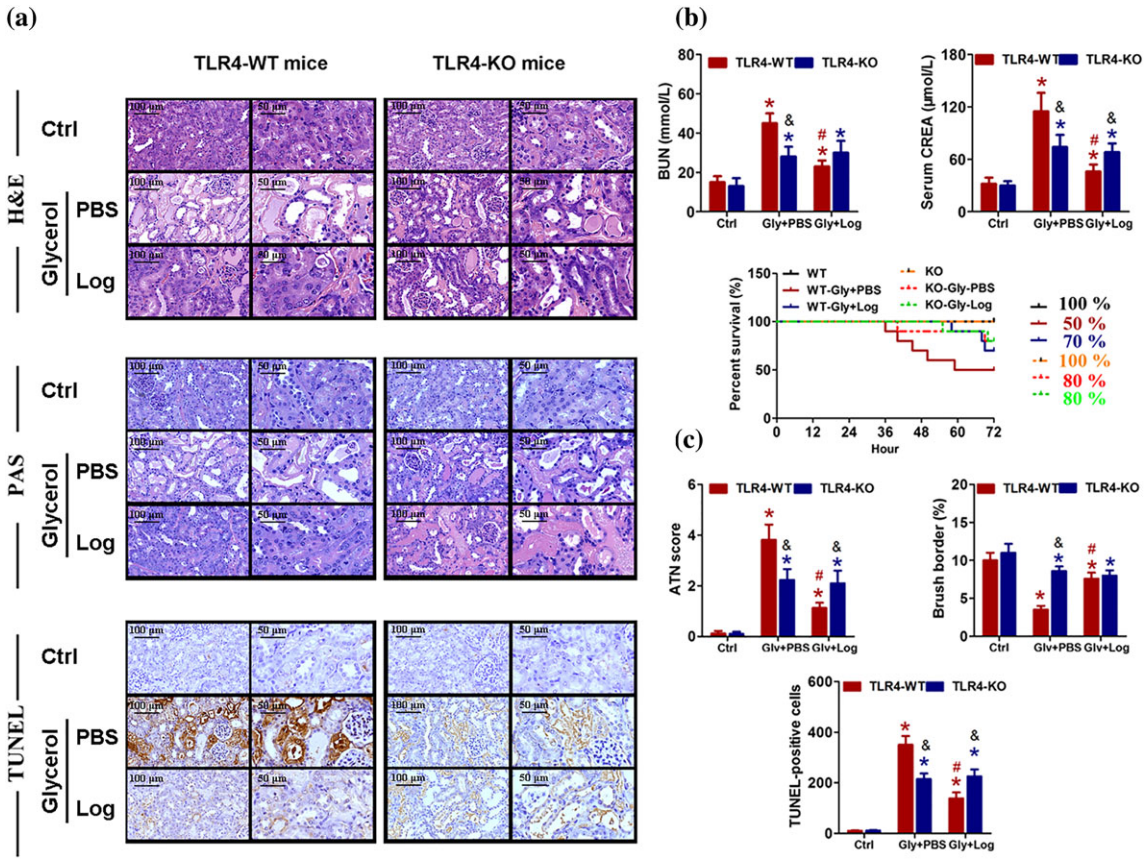

FIGURE 9 *Loganetin* improved rhabdomyolysis-induced acute kidney injury in mice by acting on the TLR4. TLR-WT and TLR-KO mice subjected to different treatments were killed at 72 hr after glycerol injection. Representative haematoxylin and eosin (upper), periodic acid-Schiff (middle), and TUNEL (lower) staining images of kidney (a), blood urea nitrogen (BUN, left), serum levels of (right) creatinine (CREA, right), and survival curves of each groups (lower) were detected and performed (b). (c) Representative images of acute tubular necrosis score, brush borders, and TUNEL-positive cells were showed. Data are expressed as means + SD, $n = 10$. *$P < 0.05$ versus control group of the same genotype; #$P < 0.05$ versus PBS group of the same genotype; &$P < 0.05$ versus the same treated group of different genotype

but was significantly ameliorated in TLR4-KO mice (Figure 9a, upper). Consistent with H&E staining, PAS and TUNEL assays showed that in wild-type mice, the ATN score, brush border, and TUNEL-positive cell were 3.82 ± 0.6, 3.5 ± 0.5, and 352 ± 34 in RIAKI mice respectively. In contrast, these parameters were 1.13 ± 0.2, 7.6 ± 0.8, and 138 ± 24 in *Loganetin*-treated RIAKI mice respectively. Additionally, *Loganetin* treatment did not affect these parameters when TLR4 was knocked out (Figure 9a, lower, c). However, the specific agonist of TLR4, LPS, partially inhibited this effect of *Loganetin*. Overall, the above results clearly demonstrated that TLR4 mediated the pathological process of RIAKI induced by glycerol injection. TLR4 depletion significantly ameliorated kidney dysfunction, renal injury, and cell death. And *Loganetin* can ameliorate RIAKI by inhibiting TLR4 activity.

4 | DISCUSSION AND CONCLUSIONS

Although there have been few studies on *Loganetin*'s bioactivity, the research on *Loganin* in general is much more widely available. It has been reported that *Loganin* can affect lipid metabolism, oxidative stress, and inflammation. *Loganin* can inhibit NF-κB activation (Kim et al., 2015). In addition, *Loganin* exhibits neuroprotection (Kwon et al., 2011), anti-amnesic activity (Lee et al., 2009), protective effects against neurodegenerative diseases (Kwon, Kim, Lee, & Jang, 2009), hepatic injury, and other diabetic complications (Yamabe et al., 2010). In Schwann SW10 cells, *Loganin* blocks the effects of TNF-α (Chao et al., 2017). *Loganetin* is produced by the deglucosylation of *Loganin* (Miettinen et al., 2014). Therefore, we speculated that the two may have similar biological functions.

Loganin has anti-inflammatory and immune-regulatory activities (Yamabe et al., 2010). In this study, we evaluated the effects of *Loganetin* on a glycerol-induced AKI mouse model. *Loganetin* efficiently improved the symptoms of AKI. Treatment with *Loganetin* resulted in decreased levels of BUN and serum CREA in AKI mice. Both high and low doses of *Loganetin* prolonged the lifespan of AKI mice. *Loganetin* prevented the apoptosis of renal tubular epithelial cells. It has been reported that *Loganin* effectively inhibits H_2O_2-induced SH-SY5Y apoptosis, and the protective mechanism has been attributed to decrease apoptosis as a result of p38, caspase-3, and cytochrome c regulation (Kao et al., 2017). We found that *Loganetin* suppressed apoptosis in the corticomedullary junction of kidney tissue in the AKI model. Our investigation of the mechanism found that 50%

glycerol resulted in an elevation of p-p65, p-JNK, p-p38, p21, and c-Jun protein levels, whereas *Loganetin* reduced these protein levels. In the mouse model, *Loganetin* treatment decreased the expression of inflammatory factors, including TNF-α, IFN-γ, and IL-17A. And *Loganetin* also reduced the infiltration of CD3+ T cells, CD45+ immune cells, and CD11b + F4/80 macrophages into the kidney (Huang et al., 2017). Glycerol-induced AKI increased the expression of TNF-α, IFN-γ, IL-6, IL-17, and IL-1β in both peripheral blood and kidney tissue. These results are in agreement with the those obtained previously (Wu et al., 2017). TNF-α and IL-6 could trigger the release of other pro-inflammatory cytokines and inflammatory mediators. IFN-γ, IL-17, and IL-1β are all involved in kidney injury (Li et al., 2010). These inflammatory factors aggravate kidney injury. Therefore, we determined the levels of these inflammatory cytokines and found that *Loganetin* inhibited their expression and ameliorated kidney injury.

In HK-2 cells, we showed that TLR4 plays a central role in AKI development. To imitate the pathological process of AKI in vitro, HK-2 cells were stimulated with LPS. *Loganetin* pretreatment markedly inhibited LPS-induced expression of p-p65, p-JNK, p-p38, p21, and c-Jun proteins. When TLR4 was knocked down by specific shRNA in the presence of LPS, *Loganetin* treatment did not alter the phosphorylation of p65, JNK, and p38 and did not affect the expression of p21, c-Jun, Bax, or caspase 3, which suggests that TLR4 plays an important role in the effects of *Loganetin* on apoptosis induced by LPS in HK-2 cells. Also *Loganetin*, pre- or post-treatment, protected HK-2 cells from apoptosis. In TLR4 knockout (TLR4-KO) mice, *Loganetin* did not display a protective effect on glycerol-induced AKI. The levels of BUN and serum CREA were not restored by *Loganetin* treatment, and the ATN score, brush border, and apoptosis in kidneys of glycerol-stimulated TLR4-KO mice were not ameliorated by *Loganetin* treatment compared with TLR4-WT mice. *Loganetin* increased the survival of glycerol-treated mice with AKI but not of the glycerol-treated TLR4-KO mice.

Novel inhibitors of TLR4 have been designed and synthesized according to the structure of the molecule, including TAK-242, which disrupts the interactions of TLR4 with its adaptor molecules (Matsunaga, Tsuchimori, Matsumoto, & Ii, 2011). Here, we report, for the first time, a natural small molecular product, *Loganetin*, which can significantly inhibit NF-κB activity by acting on TLR4. However, the exact binding site is still not clear and needs further study.

ACKNOWLEDGEMENTS

This study was supported by the National Natural Science Foundation of China (Grants 81400752 to C.Y.; 81370852 to M.X.; 81270832 to R.R.; and 81270833 and 81570674 to T.Z.).

AUTHOR CONTRIBUTIONS

Y.R., G.Z., and J.Y. contributed to the conception and design of the study and approved the final version to be submitted. J.L. contributed to drafting the article and data analysis and interpretation. Y.T., M.W., and G.L. performed samples collection from experimental animals. Y.T., and J.L. performed H&E, PAS, TUNEL, immunohistochemistry, and immunofluorescence staining. Q.W., Y.S., Z.L., and J.Y. performed ELISA and immunoblot analysis.

CONFLICT OF INTEREST

The authors declare no conflicts of interest.

DECLARATION OF TRANSPARENCY AND SCIENTIFIC RIGOUR

This Declaration acknowledges that this paper adheres to the principles for transparent reporting and scientific rigour of preclinical research as stated in the BJP guidelines for **Design & Analysis**, **Immunoblotting and Immunochemistry**, and **Animal Experimentation**, and as recommended by funding agencies, publishers and other organisations engaged with supporting research.

ORCID

Jiang Yue https://orcid.org/0000-0001-8906-1253
Yu-shan Ren https://orcid.org/0000-0003-4982-648X

REFERENCES

Alexander, S. P. H., Fabbro, D., Kelly, E., Marrion, N. V., Peters, J. A., Faccenda, E., … Collaborators, C. G. T. P. (2017a). 2017/18: Catalytic receptors. *British Journal of Pharmacology*, *174*(S1), S225–S271. https://doi.org/10.1111/bph.13876

Alexander, S. P. H., Fabbro, D., Kelly, E., Marrion, N. V., Peters, J. A., Faccenda, E., … Collaborators, C. G. T. P. (2017b). The Concise Guide to PHARMACOLOGY 2017/18: Enzymes. *British Journal of Pharmacology*, *174*(S1), S272–S359. https://doi.org/10.1111/bph.13877

Alexander, S. P., Kelly, E., Marrion, N. V., Peters, J. A., Faccenda, E., Harding, S. D., … CGTP Collaborators (2017). The Concise Guide to PHARMACOLOGY 2017/18: Overview. *British Journal of Pharmacology*, *174*(Suppl 1), S1–S16.

Arora, M. K., & Singh, U. K. (2014). Oxidative stress: Meeting multiple targets in pathogenesis of diabetic nephropathy. *Current Drug Targets*, *15*(5), 531–538. https://doi.org/10.2174/1389450115666140321120635

Ashall, V., & Millar, K. (2014). Endpoint matrix: A conceptual tool to promote consideration of the multiple dimensions of humane endpoints. *ALTEX*, *31*(2), 209–213. https://doi.org/10.14573/altex.1307261

Bellomo, R., Kellum, J. A., & Ronco, C. (2012). Acute kidney injury. *Lancet*, *380*(9843), 756–766. https://doi.org/10.1016/S0140-6736(11)61454-2

Campbell, M. T., Hile, K. L., Zhang, H., Asanuma, H., Vanderbrink, B. A., Rink, R. R., & Meldrum, K. K. (2011). Toll-like receptor 4: A novel signaling pathway during renal fibrogenesis. *The Journal of Surgical Research*, *168*(1), e61–e69. https://doi.org/10.1016/j.jss.2009.09.053

Chao, G., Tian, X., Zhang, W., Ou, X., Cong, F., & Song, T. (2017). Blocking Smad2 signalling with loganin attenuates SW10 cell cycle arrest induced by TNF-alpha. *PLoS ONE*, *12*(5), e0176965. https://doi.org/10.1371/journal.pone.0176965

Chen, J., John, R., Richardson, J. A., Shelton, J. M., Zhou, X. J., Wang, Y., … Lu, C. Y. (2011). Toll-like receptor 4 regulates early endothelial activation during ischemic acute kidney injury. *Kidney International*, *79*(3), 288–299. https://doi.org/10.1038/ki.2010.381

Curtis, M. J., Alexander, S., Cirino, G., Docherty, J. R., George, C. H., Giembycz, M. A., … Ahluwalia, A. (2018). Experimental design and analysis and their reporting II: Updated and simplified guidance for authors and peer reviewers. *British Journal of Pharmacology*, *175*(7), 987–993. https://doi.org/10.1111/bph.14153

El-Achkar, T. M., Huang, X., Plotkin, Z., Sandoval, R. M., Rhodes, G. J., & Dagher, P. C. (2006). Sepsis induces changes in the expression and distribution of Toll-like receptor 4 in the rat kidney. *American Journal of Physiology. Renal Physiology*, *290*(5), F1034–F1043. https://doi.org/10.1152/ajprenal.00414.2005

Harding, S. D., Sharman, J. L., Faccenda, E., Southan, C., Pawson, A. J., Ireland, S., … NC-IUPHAR (2018). The IUPHAR/BPS Guide to PHARMACOLOGY in 2018: Updates and expansion to encompass the new guide to IMMUNOPHARMACOLOGY. *Nucleic Acids Research*, *46*(D1), D1091–D1106. https://doi.org/10.1093/nar/gkx1121

Huang, R., Shi, M., Guo, F., Feng, Y., Liu, J., Li, L., … Fu, P. (2018). Pharmacological Inhibition of fatty acid-binding protein 4 (FABP4) protects against rhabdomyolysis-induced acute kidney injury. *Frontiers in Pharmacology*, *9*, 917. https://doi.org/10.3389/fphar.2018.00917

Huang, R. S., Zhou, J. J., Feng, Y. Y., Shi, M., Guo, F., Gou, S. J., … Fu, P. (2017). Pharmacological inhibition of macrophage Toll-like receptor 4/nuclear factor-kappa B alleviates rhabdomyolysis-induced acute kidney injury. *Chinese Medical Journal*, *130*(18), 2163–2169. https://doi.org/10.4103/0366-6999.213406

Jang, H. R., Ko, G. J., Wasowska, B. A., & Rabb, H. (2009). The interaction between ischemia-reperfusion and immune responses in the kidney. *Journal of Molecular Medicine (Berl)*, *87*(9), 859–864. https://doi.org/10.1007/s00109-009-0491-y

Jesinkey, S. R., Funk, J. A., Stallons, L. J., Wills, L. P., Megyesi, J. K., Beeson, C. C., & Schnellmann, R. G. (2014). Formoterol restores mitochondrial and renal function after ischemia-reperfusion injury. *Journal of the American Society of Nephrology: JASN*, *25*(6), 1157–1162. https://doi.org/10.1681/ASN.2013090952

Kao, C. J., Chen, W. F., Guo, B. L., Feng, C. W., Hung, H. C., Yang, W. Y., … Wen, Z. H. (2017). The 1-tosylpentan-3-one protects against 6-hydroxydopamine-induced neurotoxicity. *International Journal of Molecular Sciences*, *18*(5). https://doi.org/10.3390/ijms18051096

Kilkenny, C., Browne, W., Cuthill, I. C., Emerson, M., & Altman, D. G. (2010). Animal research: Reporting in vivo experiments: The ARRIVE guidelines. *British Journal of Pharmacology*, *160*, 1577–1579.

Kim, M. G., Koo, T. Y., Yan, J. J., Lee, E., Han, K. H., Jeong, J. C., … Yang, J. (2013). IL-2/anti-IL-2 complex attenuates renal ischemia-reperfusion injury through expansion of regulatory T cells. *Journal of the American Society of Nephrology: JASN*, *24*(10), 1529–1536. https://doi.org/10.1681/ASN.2012080784

Kim, M. J., Bae, G. S., Jo, I. J., Choi, S. B., Kim, D. G., Shin, J. Y., … Park, S. J. (2015). Loganin protects against pancreatitis by inhibiting NF-kappaB activation. *European Journal of Pharmacology*, *765*, 541–550. https://doi.org/10.1016/j.ejphar.2015.09.019

Kwon, S. H., Kim, H. C., Lee, S. Y., & Jang, C. G. (2009). Loganin improves learning and memory impairments induced by scopolamine in mice. *European Journal of Pharmacology*, *619*(1–3), 44–49. https://doi.org/10.1016/j.ejphar.2009.06.062

Kwon, S. H., Kim, J. A., Hong, S. I., Jung, Y. H., Kim, H. C., Lee, S. Y., & Jang, C. G. (2011). Loganin protects against hydrogen peroxide-induced apoptosis by inhibiting phosphorylation of JNK, p38, and ERK 1/2 MAPKs in SH-SY5Y cells. *Neurochemistry International*, *58*(4), 533–541. https://doi.org/10.1016/j.neuint.2011.01.012

Lee, K. Y., Sung, S. H., Kim, S. H., Jang, Y. P., Oh, T. H., & Kim, Y. C. (2009). Cognitive-enhancing activity of loganin isolated from Cornus officinalis in scopolamine-induced amnesic mice. *Archives of Pharmacal Research*, *32*(5), 677–683. https://doi.org/10.1007/s12272-009-1505-6

Li, J., Wan, Y., Na, S., Liu, X., Dong, G., Yang, Z., … Yue, J. (2015). Sex-dependent regulation of hepatic CYP3A by growth hormone: Roles of HNF6, C/EBPalpha, and RXRalpha. *Biochemical Pharmacology*, *93*(1), 92–103. https://doi.org/10.1016/j.bcp.2014.10.010

Li, J., Xie, M., Wang, X., Ouyang, X., Wan, Y., Dong, G., … Yue, J. (2015). Sex hormones regulate cerebral drug metabolism via brain miRNAs: Down-regulation of brain CYP2D by androgens reduces the analgesic effects of tramadol. *British Journal of Pharmacology*, *172*(19), 4639–4654. https://doi.org/10.1111/bph.13206

Li, L., Huang, L., Vergis, A. L., Ye, H., Bajwa, A., Narayan, V., … Okusa, M. D. (2010). IL-17 produced by neutrophils regulates IFN-gamma-mediated neutrophil migration in mouse kidney ischemia-reperfusion injury. *The Journal of Clinical Investigation*, *120*(1), 331–342. https://doi.org/10.1172/JCI38702

Li, P. K., Burdmann, E. A., & Mehta, R. L. (2013). World Kidney Day 2013: Acute kidney injury-global health alert. *American Journal of Kidney Diseases: The Official Journal of the National Kidney Foundation*, *61*(3), 359–363. https://doi.org/10.1053/j.ajkd.2013.01.002

Li, Y., Li, Z., Shi, L., Zhao, C., Shen, B., Tian, Y., & Feng, H. (2016). Loganin inhibits the inflammatory response in mouse 3T3L1 adipocytes and mouse model. *International Immunopharmacology*, *36*, 173–179. https://doi.org/10.1016/j.intimp.2016.04.026

Liu, K., Xu, H., Lv, G., Liu, B., Lee, M. K., Lu, C., … Wu, Y. (2015). Loganin attenuates diabetic nephropathy in C57BL/6J mice with diabetes induced by streptozotocin and fed with diets containing high level of advanced glycation end products. *Life Sciences*, *123*, 78–85. https://doi.org/10.1016/j.lfs.2014.12.028

Matsunaga, N., Tsuchimori, N., Matsumoto, T., & Ii, M. (2011). TAK-242 (resatorvid), a small-molecule inhibitor of Toll-like receptor (TLR) 4 signaling, binds selectively to TLR4 and interferes with interactions between TLR4 and its adaptor molecules. *Molecular Pharmacology*, *79*(1), 34–41. https://doi.org/10.1124/mol.110.068064

Mehta, R. L., Burdmann, E. A., Cerda, J., Feehally, J., Finkelstein, F., Garcia-Garcia, G., … Remuzzi, G. (2016). Recognition and management of acute kidney injury in the International Society of Nephrology 0by25 Global Snapshot: A multinational cross-sectional study. *Lancet*, *387*(10032), 2017–2025. https://doi.org/10.1016/S0140-6736(16)30240-9

Miettinen, K., Dong, L., Navrot, N., Schneider, T., Burlat, V., Pollier, J., … Werck-Reichhart, D. (2014). The seco-iridoid pathway from Catharanthus roseus. *Nature Communications*, *5*, 3606. https://doi.org/10.1038/ncomms4606

Nagatoshi, M., Terasaka, K., Nagatsu, A., & Mizukami, H. (2011). Iridoid-specific glucosyltransferase from Gardenia jasminoides. *The Journal of Biological Chemistry*, *286*(37), 32866–32874. https://doi.org/10.1074/jbc.M111.242586

Okamura, D. M., & Pennathur, S. (2015). The balance of powers: Redox regulation of fibrogenic pathways in kidney injury. *Redox Biology*, *6*, 495–504. https://doi.org/10.1016/j.redox.2015.09.039

Press, A. T., Butans, M. J., Haider, T. P., Weber, C., Neugebauer, S., Kiehntopf, M., … Kortgen, A. (2017). Fast simultaneous assessment of renal and liver function using polymethine dyes in animal models of chronic and acute organ injury. *Scientific Reports*, *7*(1), 15397. https://doi.org/10.1038/s41598-017-14987-5

Pulskens, W. P., Teske, G. J., Butter, L. M., Roelofs, J. J., van der Poll, T., Florquin, S., & Leemans, J. C. (2008). Toll-like receptor-4 coordinates the innate immune response of the kidney to renal ischemia/reperfusion injury. *PLoS ONE*, *3*(10), e3596. https://doi.org/10.1371/journal.pone.0003596

Ren, Y., Min, Y. Q., Liu, M., Chi, L., Zhao, P., & Zhang, X. L. (2016). *N*-Glycosylation-mutated HCV envelope glycoprotein complex enhances antigen-presenting activity and cellular and neutralizing antibody responses. *Biochimica et Biophysica Acta*, *1860*(8), 1764–1775. https://doi.org/10.1016/j.bbagen.2015.08.007

Souza, A. C., Tsuji, T., Baranova, I. N., Bocharov, A. V., Wilkins, K. J., Street, J. M., … Star, R. A. (2015). TLR4 mutant mice are protected from renal fibrosis and chronic kidney disease progression. *Physiological Reports*, *3*(9), e12558. https://doi.org/10.14814/phy2.12558

Uchino, S., Kellum, J. A., Bellomo, R., Doig, G. S., Morimatsu, H., Morgera, S., … Beginning and ending supportive therapy for the kidney (BEST Kidney) investigators (2005). Acute renal failure in critically ill patients: A multinational, multicenter study. *Jama*, *294*(7), 813–818. https://doi.org/10.1001/jama.294.7.813

Valko, M., Jomova, K., Rhodes, C. J., Kuca, K., & Musilek, K. (2016). Redox- and non-redox-metal-induced formation of free radicals and their role in human disease. *Archives of Toxicology*, *90*(1), 1–37. https://doi.org/10.1007/s00204-015-1579-5

Wang, J., Li, H., Qiu, S., Dong, Z., Xiang, X., & Zhang, D. (2017). MBD2 upregulates miR-301a-5p to induce kidney cell apoptosis during vancomycin-induced AKI. *Cell Death & Disease*, *8*(10), e3120. https://doi.org/10.1038/cddis.2017.509

Wang, S., Zhang, C., Li, J., Niyazi, S., Zheng, L., Xu, M., … Zhu, T. (2017). Erythropoietin protects against rhabdomyolysis-induced acute kidney injury by modulating macrophage polarization. *Cell Death & Disease*, *8*(4), e2725. https://doi.org/10.1038/cddis.2017.104

Wu, H., Chen, G., Wyburn, K. R., Yin, J., Bertolino, P., Eris, J. M., … Chadban, S. J. (2007). TLR4 activation mediates kidney ischemia/reperfusion injury. *The Journal of Clinical Investigation*, *117*(10), 2847–2859. https://doi.org/10.1172/JCI31008

Wu, H., Ma, J., Wang, P., Corpuz, T. M., Panchapakesan, U., Wyburn, K. R., & Chadban, S. J. (2010). HMGB1 contributes to kidney ischemia reperfusion injury. *Journal of the American Society of Nephrology: JASN*, *21*(11), 1878–1890. https://doi.org/10.1681/ASN.2009101048

Wu, J., Pan, X., Fu, H., Zheng, Y., Dai, Y., Yin, Y., … Hou, D. (2017). Effect of curcumin on glycerol-induced acute kidney injury in rats. *Scientific Reports*, *7*(1), 10114. https://doi.org/10.1038/s41598-017-10693-4

Xu, C., Chang, A., Hack, B. K., Eadon, M. T., Alper, S. L., & Cunningham, P. N. (2014). TNF-mediated damage to glomerular endothelium is an important determinant of acute kidney injury in sepsis. *Kidney International*, *85*(1), 72–81. https://doi.org/10.1038/ki.2013.286

Yamabe, N., Noh, J. S., Park, C. H., Kang, K. S., Shibahara, N., Tanaka, T., & Yokozawa, T. (2010). Evaluation of loganin, iridoid glycoside from Corni Fructus, on hepatic and renal glucolipotoxicity and inflammation in type 2 diabetic db/db mice. *European Journal of Pharmacology*, *648*(1–3), 179–187. https://doi.org/10.1016/j.ejphar.2010.08.044

Yao, L., Peng, S. X., Xu, Y. D., Lin, S. L., Li, Y. H., Liu, C. J., … Shen, Y. Q. (2017). Unexpected neuroprotective effects of loganin on 1-methyl-4-phenyl-1,2,3,6-tetrahydropyridine-induced neurotoxicity and cell death in zebrafish. *Journal of Cellular Biochemistry*, *118*(3), 615–628. https://doi.org/10.1002/jcb.25749

You, H., Gao, T., Raup-Konsavage, W. M., Cooper, T. K., Bronson, S. K., Reeves, W. B., & Awad, A. S. (2017). Podocyte-specific chemokine (C-C motif) receptor 2 overexpression mediates diabetic renal injury in mice. *Kidney International*, *91*(3), 671–682. https://doi.org/10.1016/j.kint.2016.09.042

Zhang, M. Z., Wang, X., Wang, Y., Niu, A., Wang, S., Zou, C., & Harris, R. C. (2017). IL-4/IL-13-mediated polarization of renal macrophages/dendritic cells to an M2a phenotype is essential for recovery from acute kidney injury. *Kidney International*, *91*(2), 375–386. https://doi.org/10.1016/j.kint.2016.08.020

Zhang, Q., Liu, L., Lin, W., Yin, S., Duan, A., Liu, Z., & Cao, W. (2017). Rhein reverses Klotho repression via promoter demethylation and protects against kidney and bone injuries in mice with chronic kidney disease. *Kidney International*, *91*(1), 144–156. https://doi.org/10.1016/j.kint.2016.07.040

Zhao, M., Tao, J., Qian, D., Liu, P., Shang, E. X., Jiang, S., … Du, L. (2016). Simultaneous determination of loganin, morroniside, catalpol and acteoside in normal and chronic kidney disease rat plasma by UPLC-MS for investigating the pharmacokinetics of Rehmannia glutinosa and Cornus officinalis Sieb drug pair extract. *Journal of chromatography. B, Analytical Technologies in the Biomedical and Life Sciences*, *1009-1010*, 122–129. https://doi.org/10.1016/j.jchromb.2015.12.020

Zhao, Y., Ren, Y., Zhang, X., Zhao, P., Tao, W., Zhong, J., … Zhang, X. L. (2014). Ficolin-2 inhibits hepatitis C virus infection, whereas apolipoprotein E3 mediates viral immune escape. *Journal of Immunology*, *193*(2), 783–796. https://doi.org/10.4049/jimmunol.1302563

SUPPORTING INFORMATION

Additional supporting information may be found online in the Supporting Information section at the end of the article.

How to cite this article: Li J, Tan Y, Wang M, et al. *Loganetin* protects against rhabdomyolysis-induced acute kidney injury by modulating the toll-like receptor 4 signalling pathway. *Br J Pharmacol*. 2019;176:1106–1121. https://doi.org/10.1111/bph.14595